HHS Public Access

Author manuscript

Hepatology. Author manuscript; available in PMC 2018 September 01.

Published in final edited form as:

Hepatology. 2017 September ; 66(3): 758–771. doi:10.1002/hep.29177.

Ginsenoside Rg3 Restores Hepatitis C Virus-Induced Aberrant Mitochondrial Dynamics and Inhibits Virus Propagation

Seong-Jun Kim[1,†,*], **Jae Young Jang**[2,†,*], **Eun-Jung Kim**[1], **Eun Kyung Cho**[2], **Dae Gyun Ahn**[1], **Chonsaeng Kim**[1], **Han Seul Park**[2], **Soung Won Jeong**[2], **Sae Hwan Lee**[3], **Sang Gyune Kim**[4], **Young Seok Kim**[4], **Hong Soo Kim**[3], **Boo Sung Kim**[2], **Ji-Hyung Lee**[5], and **Aleem Siddiqui**[5,6]

[1]Center for Convergent Research of Emerging Virus Infection, Korea Research Institute of Chemical Technology, Yuseong, Daejeon 34114, South Korea

[2]Institute for Digestive Research, Digestive Disease Center, Department of Internal Medicine, College of Medicine, Soonchunhyang University, Seoul 04401, South Korea

[3]Department of Internal Medicine, College of Medicine, Soonchunhyang University, Cheonan 31151, South Korea

[4]Department of Internal Medicine, College of Medicine, Soonchunhyang University, Bucheon 14584, South Korea

[5]Department of Medicine, University of California, San Diego, La Jolla, CA 92093, USA

[6]Division of Infectious Diseases, University of California, San Diego, La Jolla, CA 92093, USA

Abstract

Hepatitis C virus (HCV) alters mitochondrial dynamics associated with persistent viral infection and suppression of innate immunity. Mitochondrial dysfunction is also a pathologic feature of direct-acting antiviral (DAA) treatment. Despite the high efficacy of DAAs, their treatment of patients with chronic hepatitis C in interferon-sparing regimens occasionally produces undesirable side effects such as fatigue, migraine and other conditions, which may be linked to mitochondrial dysfunction. Here we show that clinically prescribed DAAs, including Sofosbuvir, affect mitochondrial dynamics. To counter these adverse effects, we examined HCV- and DAA-induced aberrant mitochondrial dynamics modulated by ginsenoside, which is known to support healthy mitochondrial physiology and the innate immune system. We screened several ginsenoside compounds showing antiviral activity using a robust HCV cell culture system. We investigated the role of ginsenosides in antiviral efficacy, alteration of the mitochondrial transmembrane potential, abnormal mitochondrial fission, its upstream signaling, and mitophagic process caused by HCV infection or DAA treatment. Only One of the compounds, ginsenoside Rg3 (G-Rg3), exhibited the notable and promising anti-HCV potential. Treatment of HCV-infected cells with G-Rg3 increased

[*]**Corresponding authors:** Jae Young Jang, MD, PhD, Department of Internal Medicine, College of Medicine, Soonchunhyang University, Yongsan-gu, Seoul 04401, South Korea, Phone: +82-2-7099863; Fax: +82-2-7099696; jyjang@schmc.ac.kr; Seong-Jun Kim, PhD, Center for Convergent Research of Emerging Virus Infection, Korea Research Institute of Chemical Technology, Yuseong, Daejeon 34114, South Korea, Phone: +82-42-860-7477; Fax: +82-42-861-4246; sekim@krict.re.kr.

[†]These authors contributed equally to this work.

Author contributions:

Study concept and design: S.J.K., J.Y.J.; experiments: S.J.K., J.Y.J., E.J.K., E.K.C., H.S.P., J.H.L., D.G.A., C.K.; data collection: S.W.J., S.H.L., S.G.K., Y.S.K., H.S.K., B.S.K.; data analysis: S.J.K., J.Y.J., A.S.; manuscript writing: S.J.K., J.Y.J., A.S.

HCV core protein-mediated reduction in the expression level of cytosolic p21 required for increasing the cyclin-dependent kinase 1 (CDK1) activity, which catalyzes Ser616 phosphorylation of dynamin-related protein 1 (Drp1). The HCV-induced mitophagy, which follows mitochondrial fission, was also rescued by G-Rg3 treatment.

CONCLUSIONS—G-Rg3 inhibits HCV propagation. Its antiviral mechanism involves restoring the HCV-induced Drp1-mediated aberrant mitochondrial fission process, thereby resulting in suppression of persistent HCV infection.

Keywords

New HCV treatment; Sofosbuvir; Mitochondrial dysfunction

Introduction

The hepatitis C virus (HCV) infects 2~3% of the world population and is the leading cause of hepatocellular carcinoma and end-stage liver disease requiring liver transplantation. In contrast to most other viral infections, the hallmark of HCV infection is that a majority of patients develop chronic infection after viral exposure. Unfortunately to date, an effective vaccine is not available for HCV (1).

The standard treatment option for chronic hepatitis C (CHC) patients traditionally had been a combination of pegylated interferon (IFN) and ribavirin. However, this combination treatment showed suboptimal efficacy in viral responses along with severe adverse reactions. The current standard therapy for CHC patients is direct-acting antivirals (DAAs), which has reached well-established efficacy. Telaprevir and Boceprevir are the first-wave of protease inhibitors that were introduced in 2011 (1) and currently, many second-generation DAAs specifically targeting HCV nonstructural protein (NS) 3 protease, NS5A and NS5B polymerases are being used for the treatment of CHC patients (2, 3). The application of a pegylated-IFN-free regimen with DAAs has showed very high sustained virologic response rates, up to nearly 100%, with insignificant side effects (3). Second-generation DAAs including Sofosbuvir as a monotherapy or combined Sofosbuvir and Ledipasvir are currently prevalent in clinical practice (1, 3, 4).

Sofosbuvir is an oral nucleotide analogue inhibitor that targets the HCV NS5B polymerase (1). Sofosbuvir-based IFN-free therapies for patients with HCV genotype 1 infection include Sofosbuvir or Ledipasvir with or without ribavirin for 12 weeks. Sofosbuvir plus ribavirin for 12 weeks (or 16 weeks for cirrhosis) is recommended as a treatment against HCV genotype 2 in the guidelines of both the American Association for the Study of Liver Diseases (AASLD) and the European Association for the Study of the Liver (EASL). However, the information on the clinical outcomes of these new DAAs including adverse effects and other limitations has not been reported (1, 3, 4).

Mitochondrial dynamics is crucial for the regulation of cell homeostasis (5). Mitochondria are readily damaged by various physiological changes induced by HCV infections, resulting in disruption of mitochondrial membrane potential ($\Delta\Psi_m$) and subsequent mitochondrial dysfunction followed by apoptosis (6–9). We have recently shown that HCV perturbs

mitochondrial dynamics via promoting dynamin-related protein 1 (Drp1)-mediated mitochondrial fission followed by Parkin-mediated mitophagy, which is associated with attenuation of HCV-induced apoptosis and innate immune response (8, 9).

Ginseng, as a traditional herbal medicine, has been widely used in Asian medicine (10, 11). The ginsenoside compounds in ginseng are known to exert a wide range of pharmacologic and immunologic effects (10, 11). The national center for complementary and alternative medicine, one of the centers of the US National Institutes of Health, has been supporting research aimed at obtaining a better understanding of the potential of Asian ginseng to treat various diseases, including its interactions with other herbs and drugs (12). In this study, we show that ginsenoside Rg3 (G-Rg3), one of the ginsenosides, exhibits a strong antiviral activity against HCV infection. G-Rg3 inhibits HCV-induced abnormal mitochondrial fission and mitophagy, which supports persistent viral infection. In doing so, it reverses the damage caused by viral infection when used in combination with anti-HCV DAAs. These results together reinforce the homeostatic effects of Rg3 in HCV treatment regimens.

Materials and Methods

Cell culture and virus

Human hepatoma Huh7 and Huh7.5.1 cells were grown in high-glucose DMEM (Gibco) supplemented with 10% fetal bovine serum (Gibco), 1% MEM nonessential amino acids (Gibco), 100 units/ml penicillin, and 100 μg/ml streptomycin (Gibco). The R-1 HCV subgenomic replicon cells were maintained in DMEM with 0.5 mg/ml G418 (13). Cell-culture-derived HCV JFH1 (Japanese fulminant hepatitis 1) genotype 2a (HCVcc) was propagated and prepared as described previously (14). HCV infection was performed at a multiplicity of infection (MOI) of 3.

Immunofluorescence

HCV-infected cells and those posttreated with G-Rg3 (100 μM) were grown on coverslips and used in immunofluorescence assays as described previously (8, 9, 15). For monitoring mitophagic process, Huh7 cells transfected with p-mito-mRFP-EGFP reporter were infected with HCVcc for 1 day and then treated with G-Rg3. At 2 days posttreatment, cells were immunostained with HCV core antibody. Confocal images were visualized under a 100× oil objective using an Olympus FluoView 1000 confocal microscope or Zeiss LSM700 laser scanning confocal microscope. The analyses of colocalization of proteins and mitochondrial lengths were quantified by ImageJ software and FV10-ASW 3.0 viewer software (Olympus), respectively.

Plasmids, antibodies, and reagents

The p-mito-mRFP-RFP and pFLAG-CMV-HCV core DNA plasmids used in this study were described previously (8, 15, 16). The primary antibodies used in this study include the following: rabbit monoclonal anti-Drp1 (Cell Signaling), rabbit monoclonal anti-phospho-Drp1 (Ser616) (Cell Signaling), mouse monoclonal anti-HCV core (Thermo Scientific), rabbit polyclonal anti-β-actin (Cell Signaling), mouse monoclonal anti-TOM20 (BD Biosciences), human monoclonal anti-HCV E2 (17), mouse monoclonal anti-HCV NS3

(Abcam), mouse monoclonal anti-mitofusin 2 (Mfn2) (Abcam), and rabbit polyclonal anti-VDAC1 (Cell Signaling). The secondary antibodies used for Western blot analysis were HRP-conjugated anti-mouse IgG and HRP-conjugated anti-rabbit IgG (both from Promega). The secondary antibodies for immunofluorescence were Alexa Fluor 350, 488, 594, or 647 donkey anti-mouse, rabbit, or goat IgG and Alexa Fluor 555 goat anti-human IgG (all from Molecular Probes). The chemical reagents used in this study were carbonyl cyanide *m*-chlorophenylhydrazone (CCCP) (Sigma), Sofosbuvir (Selleckchemm) and ginsenoside compounds (Sigma).

Western blot analysis

For Western blot analysis, whole cell lysates were extracted from cells, homogenized, subjected to SDS-PAGE, and transferred to a nitrocellulose membrane (Thermo Scientific). Western blot analysis with antibodies against the indicated proteins was then performed as described previously (8, 9, 15). Densitometer graphs were generated using Image J (NIH) (18).

Real-time qRT-PCR

Real-time qRT-PCR analysis of HCV RNA, ND2 and COX2 levels was performed as described previously (9).

Cell viability assay

A previously described cell viability assay (9) was used to assess the cytotoxic effects of ginsenoside compounds during HCV infection.

ΔΨm measurement

Huh7 cells infected with HCVcc or treated with Sofosbuvir, Telaprevir, Boceprevir, and CCCP at the indicated concentration were stained with JC-1 reagent (Invitrogen) for 1 h and immediately used for FACS analysis.

Human liver biopsy specimens

Frozen human liver biopsy specimens (n=6) were collected in the Soonchunhyang University Hospital Seoul from anti-HCV-negative patients (n=3) and anti-HCV-positive patients (n=3). All three anti-HCV-negative patients were nearly at the complete healing stage of drug-induced hepatitis, while all three anti-HCV-positive patients had active CHC. The liver biopsy samples were taken after obtaining written informed consent.

Statistical analysis

Statistical analyses using the unpaired Student’s t-test were performed using Sigma Plot software (Systat Software, San Jose, CA).

Results

Sofosbuvir causes aberrant mitochondrial fission

DAAs, particularly Sofosbuvir, are key components in the current IFN-sparing treatment regimens for chronic hepatitis C (CHC) patients. In spite of the high efficacy of Sofosbuvir, its role in altering mitochondrial dynamics and physiology has not been studied, although mitochondrial toxicity caused by DAAs has been reported (19). Since Sofosbuvir is an effective and one of the most widely used DAAs, we first investigated if Sofosbuvir perturbs mitochondrial dynamics associated with modulation of mitochondrial structure and function. We examined the changes in mitochondrial membrane potential ($\Delta\Psi_m$) in the presence of Sofosbuvir. Treatment of human hepatoma Huh7 cells with Sofosbuvir at the half-maximal effective concentration (EC_{50}) induced a decrease in the mitochondrial transmembrane potential ($\Delta\Psi_m$) (Fig. 1A). Similar results were obtained in cells treated with mitochondrial uncoupler carbonyl cyanide *m*-chlorophenylhydrazone (CCCP), which causes mitochondrial depolarization (Fig. 1A and Supporting Fig. S1A)(20). We also observed that Telaprevir and Boceprevir, which are HCV NS3 protease inhibitors, cause $\Delta\Psi_m$ loss (Supporting Fig. S1A). An increase in depolarized mitochondria triggers the mitochondrial recruitment of phosphorylated Drp1 (Ser616), which induces mitochondrial fission (21). As shown in Fig. 1B and Supporting Fig. S1B and C, Sofosbuvir induced distinct mitochondrial fission in human hepatoma cells, whereas dimethyl sulfoxide (DMSO)-treated cells showed typical tubular network of mitochondria (red color in the figures indicates TOM20-positive mitochondrial morphology). Telaprevir and Boceprevir also induced mitochondrial fragmentation (white color in Supporting Fig. S1B indicates MitoTracker-positive mitochondria morphology). Further, confocal microscopy revealed that the expression level of p-Drp1 (Ser616) was significantly higher in Sofosbuvir-treated cells than in DMSO-treated control cells as indicated by the p-Drp1 (Ser616) intensity immunostained green in Fig. 1B. More importantly, Sofosbuvir promoted mitochondrial recruitment of p-Drp1 (Ser616), as evidenced by colocalization of p-Drp1 (Ser616) and TOM20 (yellow spots in Fig. 1B), which supported the increase in Drp1-mediated mitochondrial fission seen in Sofosbuvir-treated cells. Telaprevir and Boceprevir also induced mitochondrial translocation of p-Drp1 (Supporting Fig. S2). Sofosbuvir-induced increase in the expression level of p-Drp1 was further analyzed by Western blot assays using whole cell lysates extracted from hepatoma cells treated with Sofosbuvir (accompanying graph in Fig. 1C). Together, these results indicate that HCV inhibitors such as Sofosbuvir, Telaprevir, and Boceprevir induce loss of $\Delta\Psi_m$ followed by mitochondrial translocation of p-Drp1 (Ser616), which promotes Drp1-mediated mitochondrial fission.

G-Rg3 inhibits HCV propagation

Cytoprotective effects of aspects of ginsenosides have been implicated in the treatment of many diseases including bacterial and viral infections (11). Furthermore, its effects on mitochondrial dynamics has also been reported (22, 23). We reasoned that these cytoprotective roles of ginsenosides may counter the adverse effects of antiviral DAAs seen in patients under treatment.

To investigate the antiviral effect of ginsenosides in HCV infected cells, we first screened several representative ginsenoside compounds isolated from the root of Korean red ginseng (*Panax ginseng* C.A. Meyer) (10). To conduct *in vitro* screening with ginsenoside compounds, we established an *in vitro* HCV infection system using HCVcc (24) and the Huh7.5.1, a highly permissive cell line for HCV infection (25). The infectivity of HCVcc in Huh7.5.1 cells was confirmed using confocal microscopy and immunostaining with an antibody specific to HCV core protein (Fig. 2A).

These analyses revealed that G-Rg3 remarkably suppresses the level of HCV RNA, as determined by real-time qRT-PCR with primers specific to the HCV 5′-untranslated region (Fig. 2B). Also, Western blot and cell viability assays showed that G-Rg3 reduces the expression level of HCV core protein in HCV-infected cells without cellular cytotoxicity (Fig. 2C and D). However, treatment of HCV-infected cells with G-Rh2, which is a protopanaxadiol type of ginsenoside like G-Rg3, induced very high cytotoxicity (Fig. 2E). These results suggest that G-Rg3 effectively inhibited HCV propagation.

G-Rg3 restores HCV-induced aberrant mitochondrial fission

We have recently shown that HCV induces Drp1-mediated mitochondrial fission, which promotes robust HCV propagation (8). To examine an inhibitory mechanism of G-Rg3 in robust HCV infections, we analyzed the role of G-Rg3 in $\Delta\Psi_m$ loss caused by HCV infection (6, 26), because the HCV-induced loss of $\Delta\Psi_m$ leads to mitochondrial fission (6, 8, 26). It is known that G-Rg3 inhibits the opening of mitochondrial permeability transition pores by free radical scavenging action (27). Consistent with our previous study (6), HCV infection decreased $\Delta\Psi_m$ compared to uninfected cells (Fig. 3A) (28, 29). Further, the HCV-induced loss of $\Delta\Psi_m$ was remarkably restored by G-Rg3 treatment (third panel and accompanying graph in Fig. 3A). We also observed that G-Rg3 restored the $\Delta\Psi_m$ loss caused by DAA treatment (Supporting Fig. S1A).

We next investigated if G-Rg3 affects HCV-induced aberrant mitochondrial fission. Consistent with our previous results (8), HCV infection induced mitochondrial fission (second panel in Fig. 3B), whereas confocal microscopic analysis of uninfected cells using immunostaining with MitoTracker displayed the typical tubular network of mitochondria (first panel in Fig. 3B). Interestingly, the G-Rg3 treatment inhibited HCV-induced mitochondrial fission formation and displayed normal tubular mitochondrial network (third panel in Fig. 3B). This effect is similar to silencing the mitochondrial fission factor (Mff) or Drp1 and resulting in mitochondrial fusion status (8). The accompanying graph in Fig. 3B indicates the restoring effect of G-Rg3 using quantification data of the mitochondrial length during HCV infection. The present data demonstrate that G-Rg3 prevented the HCV-induced loss of $\Delta\Psi_m$ and inhibited HCV-induced aberrant mitochondrial fission.

G-Rg3 suppresses HCV propagation via downregulation of Drp1

We have previously shown that HCV induces mitochondrial translocation of p-Drp1 leading to mitochondrial fission (8). Therefore, we used confocal microscopy to further examine whether G-Rg3 inhibits mitochondrial translocation of p-Drp1. As indicated by the yellow spots in the zoomed image of the third panel in Fig. 4A, HCV-infected cells showed

activation and translocation of p-Drp1 onto fragmented mitochondria. In contrast, HCV-infected cells treated with G-Rg3 displayed no translocation of p-Drp1 on the tubular mitochondrial network (red mitochondrial morphology in the zoomed image of the fourth panel in Fig. 4A). The accompanying graph in Fig. 4A shows the quantitative colocalization of p-Drp1 and mitochondrial marker TOM20.

Drp1 translocation to mitochondrial requires that Drp1 is phosphorylated at Ser616 position. We analyzed the expression level of Drp1 (S616) using whole cell lysates prepared from HCV-infected cells treated with G-Rg3. Analysis of these lysates shows that HCV infected cells treated with G-Rg3 display decreased level of Drp1 phosphorylation (Fig. 4B). There was also a modest reduction in the expression levels of Drp1 protein in these lysates. Together, these data suggest that G-Rg3 regulates Drp1 phosphorylation and subsequent mitochondrial translocation, thereby preventing HCV-induced abnormal mitochondrial fission.

Since HCV-induced mitochondrial fission is associated with virus secretion (8), we investigated if G-Rg3 affects HCV secretion. We first determined whether G-Rg3 inhibits viral replication in R-1 cells harboring HCV subgenomic replicon, supporting only the HCV replication (13). As shown in Fig. 4C, G-Rg3 did not inhibit HCV replication of HCV subgenomic replicon. Thus, it is likely that inhibitory effect of G-Rg3 is associated with viral secretion but not with replication. We further examined if G-Rg3 has any synergistic anti-HCV effect in combination with a known HCV antivirals, which inhibit HCV. We chose a 50 μM concentration of Rg-3, which does not affect viral replication to evaluate its combinatorial synergic effect. Sofosbuvir and other nucleotide analogs used in this study inhibit viral replication. As shown in Fig. 4D, Rg3 treatment produced a synergic anti-HCV effect with Sofosbuvir, Telaprevir, and Boceprevir respectively and suppressed viral propagation.

G-Rg3 inhibits HCV-induced degradation of cytoplasmic p21

HCV stimulates the activity of cyclin-dependent kinase 1 (CDK1), which promotes Drp1 phosphorylation at Ser616 in the cytoplasm (8). The subsequent mitochondrial translocation of p-Drp1 mediates mitochondrial fission during HCV infection (8, 21, 30). CDK1 activity is central to Drp1 phosphorylation at Ser616 in the cytosol during HCV infection (30). To examine how HCV promotes CDK1 activity, we analyzed the expression level of the cytoplasmic p21 protein that directly inhibits CDK1 activity (31). The expression level of cytosolic p21 protein was strikingly lower in liver biopsy materials than in the control materials (see the light brown color in the cytoplasmic area in Fig. 5A). Cytoplasmic p21-positive cells are quantified in Fig. 5B, which clearly shows that HCV down-regulates cytoplasmic p21 expression to promote CDK1 activity.

To substantiate the role of G-Rg3 in down-regulated cytoplasmic p21 during HCV infection, we prepared cytosolic fraction from HCV-infected cells and analyzed by Western blot assays using an antibody specific to p21 protein. Fig. 5C shows that HCV infection caused a decrease in the expression level of cytoplasmic p21. Surprisingly, this reduction was rescued by G-Rg3 treatment.

HCV core protein is a strong inhibitor of p21 expression (32). To further investigate the role of G-Rg3 in HCV core protein-dependent regulation of cytoplasmic p21 expression during HCV infection, we isolated the cytosolic fraction from cells transiently expressing HCV core protein, and then analyzed the expression level of cytoplasmic p21 protein. Similar to the HCV-induced decrease in cytoplasmic p21 expression shown in Fig. 5C, HCV core protein dramatically reduced the expression level of cytosolic p21 (Fig. 5D). This reduction was again rescued by G-Rg3 treatment. These data collectively suggest that restoration of cytosolic p21 by G-Rg3 during HCV infection (Fig. 5C) was not due to inhibition of HCV propagation by G-Rg3 but that G-Rg3 reversed the reduction in HCV core protein-dependent cytoplasmic p21 expression during HCV infection. In sum, G-Rg3 increased p21 and decreased CDK1 activity, which has a direct bearing on Drp1 phosphorylation and mitochondrial fission.

G-Rg3 inhibits HCV-induced abnormal mitophagys

Mitochondrial fission usually triggers mitophagy orchestrated by activation of PINK1 and Parkin recruitment to the mitochondria (33). To investigate the effect of G-Rg3 on HCV-induced mitophagy, we used a novel vector containing mRFP-EGFP dual luciferase gene fused in frame with a mitochondrial targeting sequence (mito-mRFP-EGFP), as previously described (8, 15, 34) (Fig. 6A). The hybrid protein displays a yellow image when expressed in mitochondria. However, if mitochondria fuse with lysosomes to complete the process of mitophagy, only RFP (red) is expressed as EGFP (green) is unstable in the acidic environment of lysosomes and quenched off (35, 36). In cells undergoing complete mitophagy, red puncta are visible indicating the expression of this hybrid protein in the lysosomes (35, 36). Consistent with our previous observation (8, 15), HCV infection induced mitochondrial fission and mitophagy (Fig. 6B middle panel and 6C). However, in the presence of G-Rg3, mitophagy was inhibited (Fig. 6B, lower panel). During HCV infection, Parkin, the key mediator of mitophagy, recruited to the mitochondria ubiquitinates and degrades outer mitochondrial substrates like VDAC1 and Mfn2 (9). To determine the function of G-Rg3 in mitochondrial Parkin activity during HCV infection, we performed Western blotting analysis of cellular lysates using specific VDAC1 and Mfn2 antibodies. G-Rg3 prevented ubiquitin degradation of VDAC1 and Mfn2 proteins (Fig. 6D and accompanying graph). We further show that G-Rg3 inhibited the HCV-induced decreases in the gene expression of mitochondrial DNA, mitochondrially encoded NADH dehydrogenase subunit 2 (ND2) and cyclooxygenase 2 (COX2) proteins (Fig. 6E).

The effect of G-Rg3 on innate immune responses during HCV infection was also examined (supplementary Fig. 3). G-Rg3-treated cells showed comparable antiviral responses with non-treated control during HCV infection. Therefore, it is highly likely that G-Rg3 suppresses the HCV propagation, not by immune responses, but by protective role of G-Rg3 against the HCV-induced mitophagy. These results collectively suggest that G-Rg3 rescues HCV-infected cells from mitophagy.

Discussion

This is the first report on G-Rg3 as an effective and potential candidate drug for treating hepatitis C infection along with other DAAs. G-Rg3 predominantly displayed antiviral activities in HCV-infected cells. G-Rg3 restored HCV-induced aberrant mitochondrial fission and had a synergic antiviral effect in combination with Sofosbuvir, Telaprevir and Boceprevir, respectively.

Nucleotide inhibitors that were incorporated by the mitochondrial RNA polymerase inhibited mitochondrial protein synthesis and produced a corresponding decrease in the mitochondrial oxygen consumption in cells. In contrast, nucleotide inhibitors containing multiple ribose modifications, including the active forms of Mericitabine and Sofosbuvir, were poor substrates for mitochondrial RNA polymerase and did not show mitochondrial toxicity in cells (37). However, we observed unequivocal reductions in $\Delta\Psi_m$ when Sofosbuvir, Telaprevir, or Boceprevir was present at EC_{50}. An increase in depolarized mitochondria promotes mitochondrial recruitment of cytosolic p-Drp1, thereby facilitating mitochondrial fission. More importantly, Sofosbuvir promoted the mitochondrial recruitment of p-Drp1, as evidenced by the colocalization of p-Drp1 and TOM20, inducing increases in Drp1-mediated mitochondrial fission in Sofosbuvir-treated cells. Together, these mechanisms result in Sofosbuvir-induced loss of $\Delta\Psi_m$ and Drp1-mediated mitochondrial fission. Recognized adverse effects of nucleotide inhibitors include fatigue, headache, muscle ache, nausea, and insomnia, and these may be related to mitochondrial toxicity.

Mitochondrial fission is associated with robust HCV propagation, with our recent data showing that the inhibition of mitochondrial fission by silencing Drp1 and Mff suppressed HCV secretion (8). Along the same line of the inhibition of mitochondrial fission, we showed that G-Rg3 inhibits Drp1-mediated mitochondrial fission, thereby suppressing HCV secretion. A preventive effect of G-Rg3 on abnormal mitochondrial fission caused by HCV infection or on HCV inhibitors could also provide improved therapies for chronic hepatitis C. Thus, using G-Rg3 in combination with Sofosbuvir is likely to reduce the treatment costs if a regimen involving Sofosbuvir at a low concentration and G-Rg3 can be established.

In the era of DAAs, meeting the demand for effective therapies for harder-to-treat populations is a huge concern for policymakers. HCV management is required in harder-to-treat populations with DAA, which include elderly patients, patients with decompensated liver cirrhosis, renal impairment, and the emergence of resistance-associated variants. Moreover, those who do not respond to pegylated IFN plus ribavirin treatment are also difficult to treat. The high cost of DAA might reduce its accessibility to patients, thus restricting its social benefits. It may be necessary to stratify and prioritize patients based on cost-effectiveness, stage of disease, and potential gain from treatment. However, the cost of treatment might decrease as more curative drugs become licensed, and so drugs exhibiting comparable efficacy and lower cost compared to DAAs are needed.

G-Rg3 was a strong inhibitor of HCV propagation, restoring HCV-induced abnormal mitochondrial fission followed by mitophagy by inhibiting activation of the CDK1-Drp1 pathway. The CDK1 activity was modulated by cytosolic p21, and G-Rg3 restored the p21

expression level that had been suppressed by HCV core protein (Fig. 7). These observations indicate that G-Rg3 is a strong and safe suppressor of HCV infection. Its antiviral mechanism involves modulating HCV-induced aberrant mitochondrial dynamics, thereby suppressing persistent HCV infection. Also, G-Rg3 acts as a synergistic and complementary agent with nucleotide inhibitors, especially Sofosbuvir. Our data suggest that G-Rg3 is a valuable new candidate for treating HCV patients either as a monotherapy or in combination with Sofosbuvir. Possible application of G-Rg3 for other viral infections is presently being investigated (38, 39).

Despite the promising potential of G-Rg3 as a multi-functional drug candidate including anti-cancer (40), anti-angiogenesis (41), liver protection (42), immune enhancement and hypertension management, neuroprotective effect (43), there could be some concern regarding its metabolic consequence. For instance, G-Rg3 can be quickly metabolized to protopanaxadiol and G-Rh2 by bacteria in the intestinal tract with diverse intestinal microbial flora (44, 45), resulting in different clinical output depending upon an individual. In addition, G-Rh2 is known to have anti-cancer effect but can be highly toxic to normal cells (Fig. 2E). Therefore, the use of G-Rg3 compound as an antiviral should be evaluated with caution.

Supplementary Material

Refer to Web version on PubMed Central for supplementary material.

Acknowledgments

We thank Dr. Takaji Wakita (National Institute of Infectious Disease, Japan) for providing the HCV p-JFH1 plasmid, Dr. Francis V. Chisari (The Scripps Research Institute, La Jolla, CA) for providing Huh7.5.1 cells, Dr. Mansun Law (ref) (The Scripps Research Institute, La Jolla, CA) for providing the HCV E2 (AR3A) antibody, and Dr. Jong-Won Oh (Yonsei University, Seoul, Korea) for providing the R-1 HCV subgenomic replicon cells.

Grant support:

This work was supported by the Korea Research Institute of Chemical Technology (KK1603-C00), the National Research Council of Science & Technology (NST) grant by the Korea government (MSIP) (CRC-16-01-KRICT), the Soonchunhyang University Research Fund (SCH Biopharm Human Resources Development Center Foundation) and National Institutes of Health grants (AI085087 and DK077704 to A.S.).

Abbreviations

HCV	hepatitis C virus
HCVcc	cell culture-derived hepatitis C virus Japanese fulminant hepatitis 1 genotype 2a
JFH1	Japanese fulminant hepatitis 1
G-Rg3	ginsenoside Rg3
Drp1	dynamin-related protein 1
DAA	direct-acting antiviral

Mfn2	mitofusin 2
ND2	mitochondrially encoded NADH dehydrogenase subunit 2
COX2	cyclooxygenase 2
TOM20	translocase of outer mitochondrial membrane 20
$\Delta\Psi_m$	mitochondrial membrane potential
Mff	mitochondrial fission factor
mito-RFP-GFP	signal peptide targeting mitochondria–red fluorescence protein–green fluorescence protein
DMSO	dimethyl sulfoxide
CDK1	cyclin-dependent kinase 1
IFN	interferon
CHC	chronic hepatitis C
NS	nonstructural protein
MOI	multiplicity of infection
CCCP	carbonyl cyanide *m*-chlorophenylhydrazone
EC_{50}	half-maximal effective concentration
p-Drp1	dynamin-related protein 1 phosphorylated at Ser616

References

1. Rose L, Bias TE, Mathias CB, Trooskin SB, Fong JJ. Sofosbuvir: A Nucleotide NS5B Inhibitor for the Treatment of Chronic Hepatitis C Infection. Ann Pharmacother. 2014; 48:1019–1029. [PubMed: 24811396]
2. Kiser JJ, Flexner C. Direct-acting antiviral agents for hepatitis C virus infection. Annu Rev Pharmacol Toxicol. 2013; 53:427–449. [PubMed: 23140245]
3. Elbaz T, El-Kassas M, Esmat G. New era for management of chronic hepatitis C virus using direct antiviral agents: A review. J Adv Res. 2015; 6:301–310. [PubMed: 26257927]
4. Cho Y, Cho EJ, Lee JH, Yu SJ, Yoon JH, Kim YJ. Sofosbuvir-based therapy for patients with chronic hepatitis C: Early experience of its efficacy and safety in Korea. Clin Mol Hepatol. 2015; 21:358–364. [PubMed: 26770924]
5. Suen DF, Norris KL, Youle RJ. Mitochondrial dynamics and apoptosis. Genes Dev. 2008; 22:1577–1590. [PubMed: 18559474]
6. Korenaga M, Wang T, Li Y, Showalter LA, Chan T, Sun J, Weinman SA. Hepatitis C virus core protein inhibits mitochondrial electron transport and increases reactive oxygen species (ROS) production. J Biol Chem. 2005; 280:37481–37488. [PubMed: 16150732]
7. Waris G, Siddiqui A. Hepatitis C virus stimulates the expression of cyclooxygenase-2 via oxidative stress: role of prostaglandin E2 in RNA replication. J Virol. 2005; 79:9725–9734. [PubMed: 16014934]

8. Kim SJ, Syed GH, Khan M, Chiu WW, Sohail MA, Gish RG, Siddiqui A. Hepatitis C virus triggers mitochondrial fission and attenuates apoptosis to promote viral persistence. Proc Natl Acad Sci U S A. 2014; 111:6413–6418. [PubMed: 24733894]
9. Kim SJ, Syed GH, Siddiqui A. Hepatitis C virus induces the mitochondrial translocation of Parkin and subsequent mitophagy. PLoS Pathog. 2013; 9:e1003285. [PubMed: 23555273]
10. Choi KT. Botanical characteristics, pharmacological effects and medicinal components of Korean Panax ginseng C A Meyer. Acta Pharmacol Sin. 2008; 29:1109–1118. [PubMed: 18718180]
11. Dzubak P, Hajduch M, Vydra D, Hustova A, Kvasnica M, Biedermann D, Markova L, et al. Pharmacological activities of natural triterpenoids and their therapeutic implications. Nat Prod Rep. 2006; 23:394–411. [PubMed: 16741586]
12. Jia L, Zhao Y, Liang XJ. Current evaluation of the millennium phytomedicine- ginseng (II): Collected chemical entities, modern pharmacology, and clinical applications emanated from traditional Chinese medicine. Curr Med Chem. 2009; 16:2924–2942. [PubMed: 19689273]
13. Kim SJ, Kim JH, Kim YG, Lim HS, Oh JW. Protein kinase C-related kinase 2 regulates hepatitis C virus RNA polymerase function by phosphorylation. J Biol Chem. 2004; 279:50031–50041. [PubMed: 15364941]
14. Jang JY, Shao RX, Lin W, Weinberg E, Chung WJ, Tsai WL, Zhao H, et al. HIV infection increases HCV-induced hepatocyte apoptosis. J Hepatol. 2011; 54:612–620. [PubMed: 21146890]
15. Kim SJ, Khan M, Quan J, Till A, Subramani S, Siddiqui A. Hepatitis B virus disrupts mitochondrial dynamics: induces fission and mitophagy to attenuate apoptosis. PLoS Pathog. 2013; 9:e1003722. [PubMed: 24339771]
16. Waris G, Felmlee DJ, Negro F, Siddiqui A. Hepatitis C virus induces proteolytic cleavage of sterol regulatory element binding proteins and stimulates their phosphorylation via oxidative stress. J Virol. 2007; 81:8122–8130. [PubMed: 17507484]
17. Law M, Maruyama T, Lewis J, Giang E, Tarr AW, Stamataki Z, Gastaminza P, et al. Broadly neutralizing antibodies protect against hepatitis C virus quasispecies challenge. Nat Med. 2008; 14:25–27. [PubMed: 18064037]
18. Schneider CA, Rasband WS, Eliceiri KW. NIH Image to ImageJ: 25 years of image analysis. Nat Methods. 2012; 9:671–675. [PubMed: 22930834]
19. Kakuda TN. Pharmacology of nucleoside and nucleotide reverse transcriptase inhibitor-induced mitochondrial toxicity. Clin Ther. 2000; 22:685–708. [PubMed: 10929917]
20. Nieminen AL, Dawson TL, Gores GJ, Kawanishi T, Herman B, Lemasters JJ. Protection by acidotic pH and fructose against lethal injury to rat hepatocytes from mitochondrial inhibitors, ionophores and oxidant chemicals. Biochem Biophys Res Commun. 1990; 167:600–606. [PubMed: 2322245]
21. Chen H, Chan DC. Mitochondrial dynamics–fusion, fission, movement, and mitophagy–in neurodegenerative diseases. Hum Mol Genet. 2009; 18:R169–176. [PubMed: 19808793]
22. Huu Tung N, Uto T, Morinaga O, Kim YH, Shoyama Y. Pharmacological effects of ginseng on liver functions and diseases: a minireview. Evid Based Complement Alternat Med. 2012; 2012:173297. [PubMed: 22997528]
23. Sun M, Huang C, Wang C, Zheng J, Zhang P, Xu Y, Chen H, et al. Ginsenoside Rg3 improves cardiac mitochondrial population quality: mimetic exercise training. Biochem Biophys Res Commun. 2013; 441:169–174. [PubMed: 24140059]
24. Wakita T, Pietschmann T, Kato T, Date T, Miyamoto M, Zhao Z, Murthy K, et al. Production of infectious hepatitis C virus in tissue culture from a cloned viral genome. Nat Med. 2005; 11:791–796. [PubMed: 15951748]
25. Zhong J, Gastaminza P, Cheng G, Kapadia S, Kato T, Burton DR, Wieland SF, et al. Robust hepatitis C virus infection in vitro. Proc Natl Acad Sci U S A. 2005; 102:9294–9299. [PubMed: 15939869]
26. Lee SK, Park SO, Joe CO, Kim YS. Interaction of HCV core protein with 14-3-3epsilon protein releases Bax to activate apoptosis. Biochem Biophys Res Commun. 2007; 352:756–762. [PubMed: 17141194]

27. Tian J, Zhang S, Li G, Liu Z, Xu B. 20(S)-ginsenoside Rg3, a neuroprotective agent, inhibits mitochondrial permeability transition pores in rat brain. Phytother Res. 2009; 23:486–491. [PubMed: 19003949]
28. Perelman A, Wachtel C, Cohen M, Haupt S, Shapiro H, Tzur A. JC-1: alternative excitation wavelengths facilitate mitochondrial membrane potential cytometry. Cell Death Dis. 2012; 3:e430. [PubMed: 23171850]
29. Reers M, Smith TW, Chen LB. J-aggregate formation of a carbocyanine as a quantitative fluorescent indicator of membrane potential. Biochemistry. 1991; 30:4480–4486. [PubMed: 2021638]
30. Knott AB, Perkins G, Schwarzenbacher R, Bossy-Wetzel E. Mitochondrial fragmentation in neurodegeneration. Nat Rev Neurosci. 2008; 9:505–518. [PubMed: 18568013]
31. Castedo M, Perfettini JL, Roumier T, Kroemer G. Cyclin-dependent kinase-1: linking apoptosis to cell cycle and mitotic catastrophe. Cell Death Differ. 2002; 9:1287–1293. [PubMed: 12478465]
32. Lee MN, Jung EY, Kwun HJ, Jun HK, Yu DY, Choi YH, Jang KL. Hepatitis C virus core protein represses the p21 promoter through inhibition of a TGF-beta pathway. J Gen Virol. 2002; 83:2145–2151. [PubMed: 12185267]
33. Youle RJ, Narendra DP. Mechanisms of mitophagy. Nat Rev Mol Cell Biol. 2011; 12:9–14. [PubMed: 21179058]
34. Khan M, Syed GH, Kim SJ, Siddiqui A. Mitochondrial dynamics and viral infections: A close nexus. Biochim Biophys Acta. 2015; 1853:2822–2833. [PubMed: 25595529]
35. Bampton ET, Goemans CG, Niranjan D, Mizushima N, Tolkovsky AM. The dynamics of autophagy visualized in live cells: from autophagosome formation to fusion with endo/lysosomes. Autophagy. 2005; 1:23–36. [PubMed: 16874023]
36. Katayama H, Yamamoto A, Mizushima N, Yoshimori T, Miyawaki A. GFP-like proteins stably accumulate in lysosomes. Cell Struct Funct. 2008; 33:1–12. [PubMed: 18256512]
37. Feng JY, Xu Y, Barauskas O, Perry JK, Ahmadyar S, Stepan G, Yu H, et al. Role of Mitochondrial RNA Polymerase in the Toxicity of Nucleotide Inhibitors of Hepatitis C Virus. Antimicrob Agents Chemother. 2016; 60:806–817. [PubMed: 26596942]
38. Kang LJ, Choi YJ, Lee SG. Stimulation of TRAF6/TAK1 degradation and inhibition of JNK/AP-1 signalling by ginsenoside Rg3 attenuates hepatitis B virus replication. Int J Biochem Cell Biol. 2013; 45:2612–2621. [PubMed: 24004833]
39. Yoo YC, Lee J, Park SR, Nam KY, Cho YH, Choi JE. Protective effect of ginsenoside-Rb2 from Korean red ginseng on the lethal infection of haemagglutinating virus of Japan in mice. J Ginseng Res. 2013; 37:80–86. [PubMed: 23717160]
40. Shan X, Fu YS, Aziz F, Wang XQ, Yan Q, Liu JW. Ginsenoside Rg3 inhibits melanoma cell proliferation through down-regulation of histone deacetylase 3 (HDAC3) and increase of p53 acetylation. PLoS One. 2014; 9:e115401. [PubMed: 25521755]
41. Liu TG, Huang Y, Cui DD, Huang XB, Mao SH, Ji LL, Song HB, et al. Inhibitory effect of ginsenoside Rg3 combined with gemcitabine on angiogenesis and growth of lung cancer in mice. BMC Cancer. 2009; 9:250. [PubMed: 19624862]
42. Lee HU, Bae EA, Han MJ, Kim DH. Hepatoprotective effect of 20(S)-ginsenosides Rg3 and its metabolite 20(S)-ginsenoside Rh2 on tert-butyl hydroperoxide-induced liver injury. Biol Pharm Bull. 2005; 28:1992–1994. [PubMed: 16204963]
43. Tian J, Fu F, Geng M, Jiang Y, Yang J, Jiang W, Wang C, et al. Neuroprotective effect of 20(S)-ginsenoside Rg3 on cerebral ischemia in rats. Neurosci Lett. 2005; 374:92–97. [PubMed: 15644271]
44. Qian T, Cai Z. Biotransformation of ginsenosides Rb1, Rg3 and Rh2 in rat gastrointestinal tracts. Chin Med. 2010; 5:19. [PubMed: 20504301]
45. Bae EA, Han MJ, Choo MK, Park SY, Kim DH. Metabolism of 20(S)- and 20(R)-ginsenoside Rg3 by human intestinal bacteria and its relation to in vitro biological activities. Biol Pharm Bull. 2002; 25:58–63. [PubMed: 11824558]

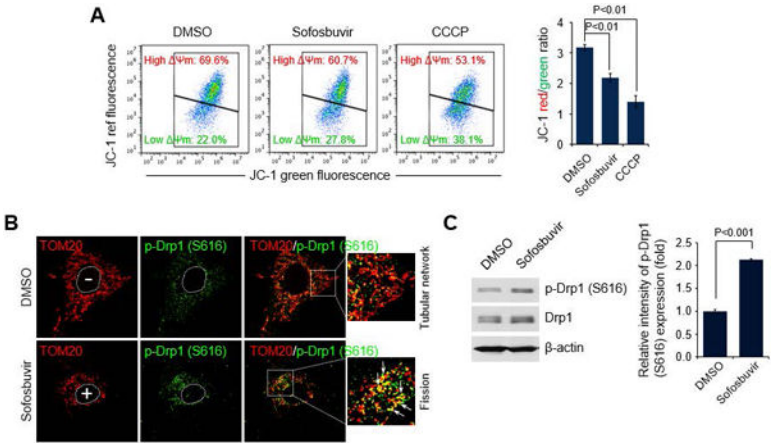

Fig. 1. Sofosbuvir induces mitochondrial damage and Drp1-mediated mitochondrial fission

(A) FACS analysis showing decrease in $\Delta\Psi_m$ in the presence of Sofosbuvir. At 24 hours after treatment with Sofosbuvir (100 nM), Huh7 cells were stained with JC-1 dye and then analyzed on a flow cytometer. The mitochondrial uncoupler CCCP (5 μM) was used as a control. The accompanying graph indicates that Sofosbuvir induced decreases in the level of $\Delta\Psi_m$, as indicated by the JC-1 red/green ratio (right panel). (B) Representative confocal microscope image showing phosphorylated Drp1 translocation to mitochondria and mitochondrial fission in the presence of Sofosbuvir. At 24 hours after treatment with Sofosbuvir (100 nM), Huh7 cells were immunostained with antibodies against TOM20 (red) and p-Drp1 (S616) (green). Nuclei are demarcated with white dotted circles. Treated (+) and untreated (–) cells are marked. In the zoomed images, the arrows indicate the colocalization of TOM20 and p-Drp1 (S616) in Sofosbuvir-treated cells (yellow spots). (C) Western blot analysis of p-Drp1 (S616) and Drp1 expression in Sofosbuvir-treated cells. Whole-cell lysates extracted from Huh7 cells treated with Sofosbuvir (100 nM) for 24 hours were analyzed by immunoblotting with antibodies specific to p-Drp1 (S616) and Drp1 proteins. β-actin was used as an internal loading control. The accompanying graph indicates that Sofosbuvir stimulates Drp1 phosphorylation (right panel).

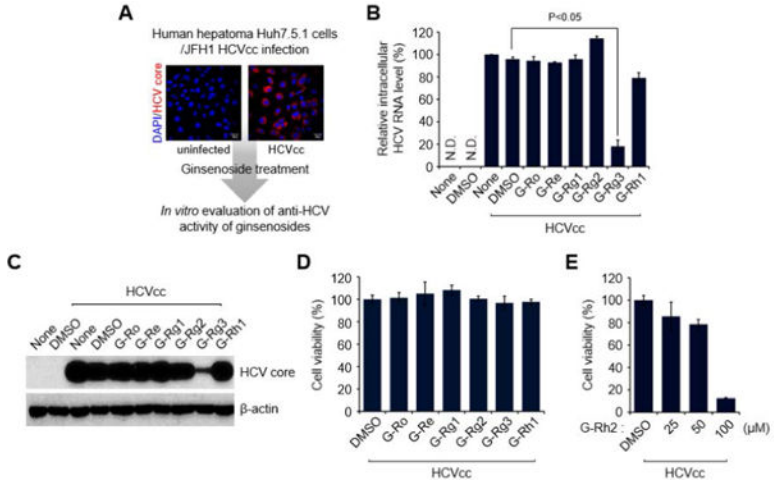

Fig. 2. G-Rg3 inhibits HCV propagation

(A) A strategy for screening ginsenosides that show antiviral effects during HCV propagation. Huh7.5.1 cells infected with JFH1 HCVcc for 1 day at an MOI of 5 were treated with various ginsenosides at 100 μM. At 2 days posttreatment, cells were harvested and used for analyses of intracellular HCV RNA (B) and protein expression (C). Confocal-microscope images show HCV core protein expression (red) in uninfected (left) and infected (right) cells. Nuclei are immunostained with DAPI (blue). (B) Intracellular HCV RNA levels were analyzed by real-time qRT-PCR as described in the Materials and Methods. GAPDH was used as the control for determining the normalized changes in HCV RNA expression. (C) Western blot analysis showing the reduction in HCV core protein expression induced by G-Rg3 treatment. Whole-cell lysates extracted from HCV-infected cells were analyzed by immunoblotting with an antibody specific to HCV core protein. (D) MTT assay data showing the viability of HCV-infected cells treated with ginsenosides for 2 days. Cell viability was measured as described in the Materials and Methods. (E) Viability of HCV-infected cells treated with G-Rh2.

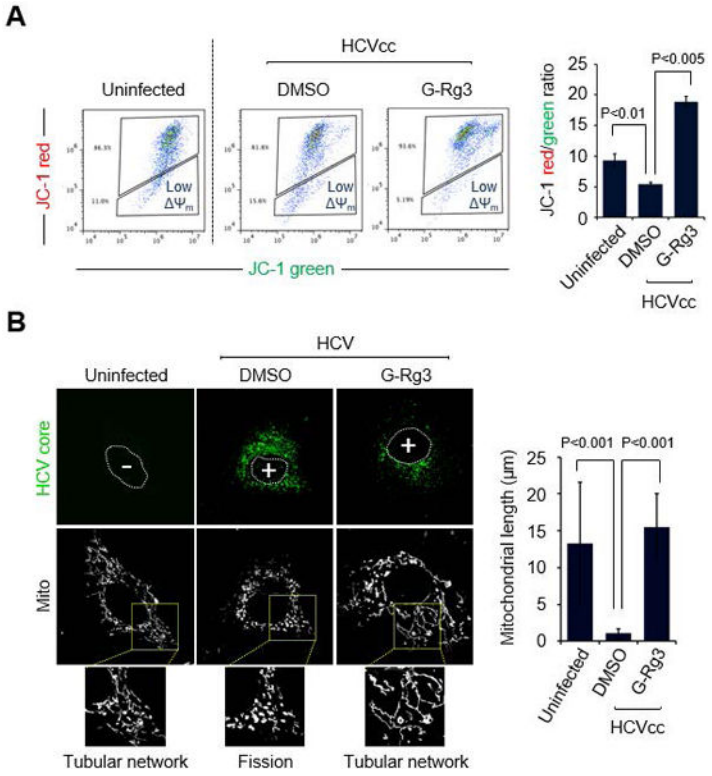

Fig. 3. G-Rg3 inhibits HCV-induced mitochondrial fission

(A) Representative FACS analysis showing restoration of HCV-induced reduction of $\Delta\Psi_m$ in the presence of G-Rg3. Cells infected with HCVcc for 1 day were treated with G-Rg3 (100 μM). At 1 day posttreatment, HCV-infected Huh7 cells were stained with JC-1 dye and then analyzed on a flow cytometer. The accompanying graph indicates that G-Rg3 restores the HCV-induced decrease in the level of $\Delta\Psi_m$, as indicated by the JC-1 red/green ratio (right panel). Data is average of two independent experiments. (B) Representative confocal images showing the mitochondrial tubular network in HCV-infected cells treated with G-Rg3. Huh7 cells infected with HCVcc at an MOI of 1 were treated with G-Rg3 (100 μM). At 1 day posttreatment, cells prestained with MitoTracker (Mito, white) were immunostained with HCV core antibody (green). Nuclei are demarcated with white dots. Infected (+) and uninfected (–) cells are marked. In the zoomed images, uninfected (left panel) and HCV-infected/G-Rg3 (right panel) cells show the typical tubular mitochondrial network, whereas HCV infected cells (middle panel) display a fragmented mitochondrial structure. The accompanying graph is quantitative analysis of the mitochondrial length in left confocal images (mean ± SEM; n = 10 mitochondria, two independent experiments).

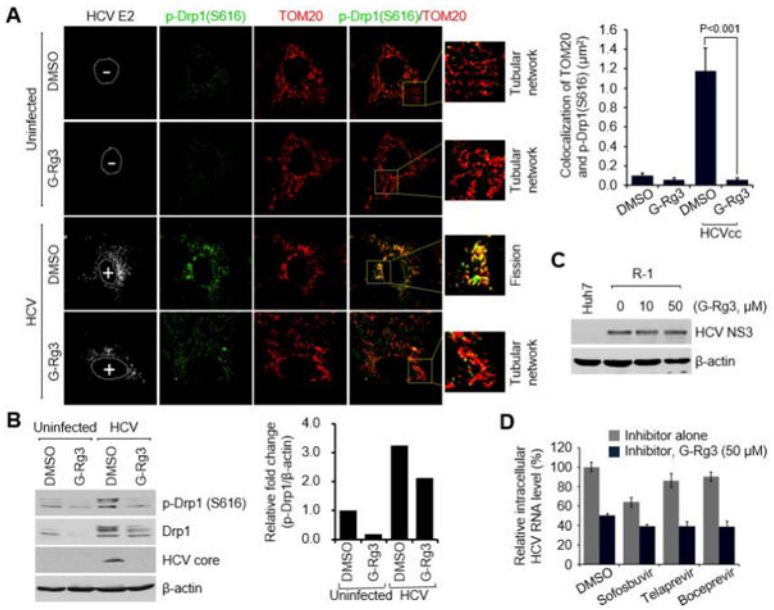

Fig. 4. G-Rg3 inhibits HCV-induced mitochondrial recruitment of Drp1

(A) Confocal-microscope images showing inhibition of Drp1 translocation to mitochondria in HCV-infected cells in the presence of G-Rg3. At 2 days after treatment with G-Rg3 (100 μM), Huh7 cells infected with HCVcc were immunostained with antibodies against TOM20 (red), p-Drp1 (S616) (green) and HCV E2 protein (white). Nuclei are demarcated with white dotted circles. Infected (+) and uninfected (–) cells are marked. In the zoomed images, the arrows indicate the colocalization of TOM20 and p-Drp1 (S616) in HCV-infected cells (yellow spots). The accompanying graph is quantitative analysis of the colocalization of TOM20 and p-Drp1 (S616) in left panel. (mean ± SEM; n = 10 mitochondria, two independent experiments). (B) Western blot analysis of p-Drp1 (S616) and Drp1 expression in HCV-infected cells treated with G-Rg3. Whole-cell lysates extracted from HCV-infected cells treated with G-Rg3 (100 μM) for 2 days were analyzed by immunoblotting with antibodies specific to p-Drp1 (S616), Drp1, and HCV core protein. β-actin was used as an internal loading control. The accompanying graph is quantitation of Western blot data in left panel. (C) Western blot analysis showing the antiviral effect of G-Rg3 in R-1 HCV subgenomic replicon cells. Whole-cell lysates of R-1 cells treated with G-Rg3 were analyzed by immunoblotting with antibodies specific to HCV NS3 protein. β-actin was used as an internal loading control. (D) HCV-infected Huh7 cells were treated with various HCV inhibitors at 10 nM (representing an approximate 10-fold dilution of EC_{50}) or in combination with G-Rg3 (50 μM). At 1 day posttreatment, cells were harvested and used for analyses of intracellular HCV RNA by real-time qRT-PCR as described in the Materials and Methods. GAPDH was used as the control for determining the normalized changes in HCV RNA expression.

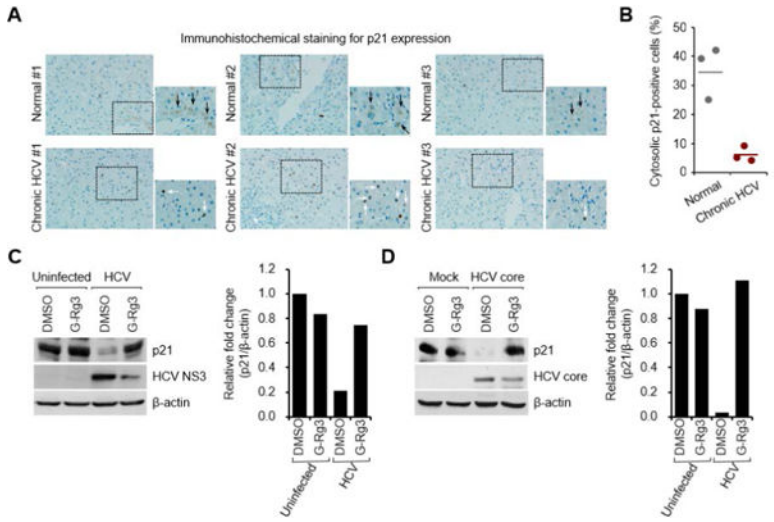

Fig. 5. G-Rg3 restores HCV-induced decrease in p21 expression

(A) Immunohistochemical analysis showing the reduction of cytosolic p21 expression in liver biopsy materials from patients with CHC. The immunohistochemical assay was performed with a specific antibody for p21 protein (dark brown). In the zoomed images, black arrows (dark brown) indicate the cytosolic expression of p21 protein, whereas white arrows indicate p21-positive staining in nuclei in HCV-infected tissue. (B) Quantitative analyses of p21-positive signals targeting the cytoplasm in panel A. (C and D) Western blot analyses showing rescue of the decreased cytosolic p21 expression level in G-Rg3-treated HCV-infected cells (C) and HCV-core-protein-transfected cells (D). The crude cytosolic fractions isolated from G-Rg3-treated HCV-infected cells (C) and HCV-core-protein-transfected cells (D) were analyzed by immunoblotting with antibodies specific to p21 and HCV core protein. β-actin was used as an internal loading control. Accompanying graphs are quantitation of Western blot data in left panel, respectively.

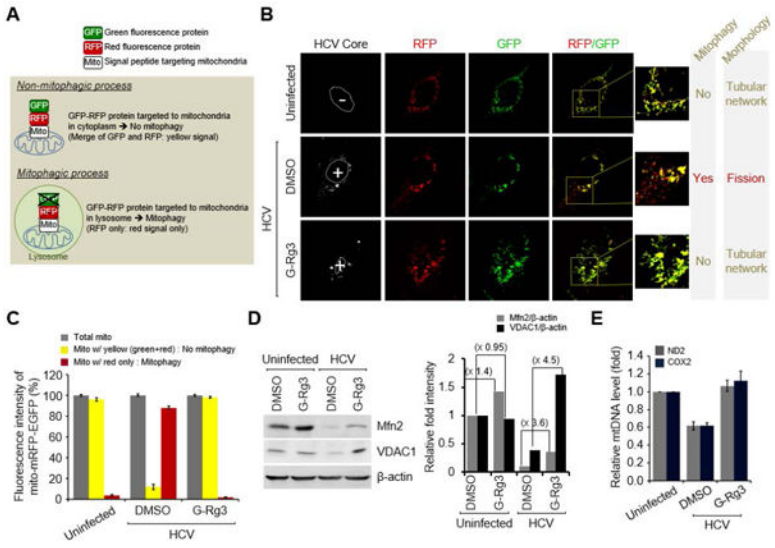

Fig. 6. G-Rg3 Inhibits HCV-induced mitophagy

(A) A system for monitoring the mitophagosomal maturation process by which mitophagosomes are delivered to lysosomes (mitophagy) using a dual fluorescence reporter/sensor, p-mito-mRFP-EGFP. Lysosomal delivery of the tandem fusion protein mito-mRFP-EGFP targeting entire mitochondria results in differential quenching and degradation of the two individual fluorochromes, thereby allowing for visual analysis of mitophagic flux. (B) Confocal microscope images showing G-Rg3-mediated inhibition of HCV-induced mitophagy. HCV-infected cells transiently expressing mito-RFP-GFP were treated with G-Rg3 (100 μM) for 48 hours and then immunostained with anti-HCV core antibody (white). Nuclei are demarcated with white dotted circles. Infected (+) and uninfected (–) cells are marked. The fluorescence signals in the zoomed images indicate the expression of mito-RFP-GFP targeting mitochondria: yellow color, no mitophagy; red color, mitophagy. (C) Quantitative analyses of the fluorescence signals targeting mitochondria in panel A. (D) Western blot analyses of Mfn2 and VDAC1 expression in HCV-infected cells treated with G-Rg3. Whole-cell lysates extracted from HCV-infected cells treated with G-Rg3 (100 μM) for 2 days were analyzed by immunoblotting with antibodies specific to Mfn2 and VDAC1 protein. β-actin was used as an internal loading control. (E) Real-time qRT-PCR analysis of mitochondrial DNA level in HCV-infected cells treated with G-Rg3. Mitochondrial ND2 and COX2 DNAs isolated from HCV-infected cells treated with G-Rg3 (100 μM) for 2 days were analyzed by real-time qRT-PCR with primers specific to ND2 and COX2 gene. β-actin was used for normalization.

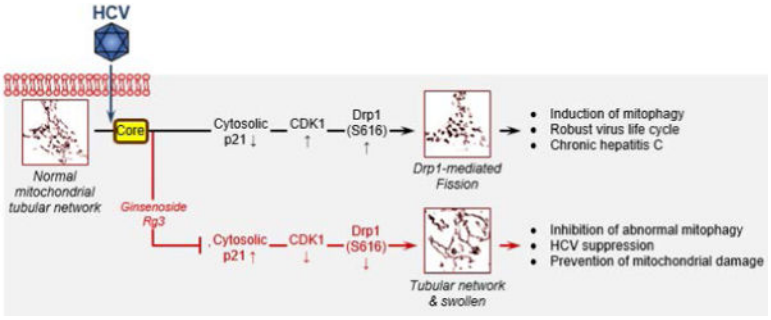

Fig. 7. Schematic of the function of G-Rg3 in mitochondrial dynamics perturbed by HCV infection

HCV infections induce endoplasmic reticulum stress and trigger calcium leakage from the endoplasmic reticulum, resulting in mitochondrial oxidative stress and an altered membrane potential, which in turn causes mitochondrial depolarization and induces mitochondrial fission initiated by the mitochondrial translocation of p-Drp1. HCV core protein induces degradation of cytosolic p21 expression that leads to up-regulation in CDK1 and p-Drp1 that can be modulated by G-Rg3 treatment.